Infrared Intensities of ν(Si−H) on H/Si(100)-2×1: Effect of O Incorporation and Agglomeration

Mathew D. Halls and Krishnan Raghavachari*

Department of Chemistry, Indiana University, Bloomington, Indiana 47405

Received: July 19, 2004; In Final Form: October 1, 2004

Hybrid density functional calculations have been carried out on cluster models of the pristine and oxidized hydrogen-terminated Si(100)-2×1 surface to investigate the changes in the surface infrared absorption spectrum upon incorporation of oxygen. Due to a combination of geometric and electronic effects, a dramatic increase in the ν(Si−H) band intensity is found for the oxidized surface. An increase in infrared intensity of up to 62% is predicted for multiply oxidized sites. The results presented here may prompt the reinterpretation of infrared studies examining silicon surface chemistry using the ν(Si−H) region to probe changes in surface structure and coverage.

I. Introduction

Vibrational spectroscopy is one of the most powerful and widely used tools in semiconductor materials research. In particular, infrared (IR) absorption spectroscopy has grown to be an invaluable tool, providing insight into critical aspects of silicon surface structure and reactivity. Changes in the surface infrared spectrum upon reactive exposure can be used to extract information concerning the chemical identity, surface coverage, and dynamic properties of the surface layer through analysis of the vibrational frequencies, band intensities, and line shapes.[1] An illustrative example of the central role infrared spectroscopy plays in understanding silicon surface chemistry is the discovery and understanding of the HF-etching chemical method for producing atomically smooth ideally hydrogen-terminated Si(111) surfaces.[2−4]

The H/Si surface infrared spectrum contains a central wavenumber region with substantial intensity between 2000 and 2300 cm^{-1}, corresponding to Si−H stretching modes (ν(Si−H)) which are an often used diagnostic probe of the H/Si surface structure. The spectral complexity in this region is indicative of the nature of the H/Si surface under examination and reflects characteristics such as the density of structural defects and the degree of hydrogen monolayer coverage. For atomically flat H-terminated Si(111) surfaces, this region is composed of a single sharp absorption line at ca. 2084 cm^{-1}, whereas for atomically rough H/Si(100) surfaces the spectrum is typically much more complex due to the presence of dihydride and trihydride surface species, in addition to the monohydride-terminated sites. The assignment and understanding of the characteristic ν(Si−H) modes for hydrogen-terminated Si(111) and Si(100) surfaces has benefited greatly by insight furnished by quantum chemical calculations.[5−8]

The oxidation of silicon continues to receive an immense amount of attention due to the widespread use of SiO_2 films as insulating layers in microelectronics, and the increasing interest in limiting silicon oxidation at silicon/high-κ metal oxide interfaces.[9] The structural and chemical evolution of hydrogen-terminated silicon surfaces during oxidation through exposure to an oxygen precursor, such as H_2O, O_2, or O_3, is commonly followed using infrared absorption spectroscopy.[10−14] Various surface reaction pathways are available to the chemical system during such a treatment with many potentially leading to a loss or even gain of surface hydrogens. Quantification of the change in surface hydrogen monolayer coverage involves careful examination of the total infrared band intensities in the characteristic ν(Si−H) region. To date, studies analyzing such changes in surface hydride structure and coverage have assumed that the intrinsic ν(Si−H) infrared intensity is conserved between pristine and oxidized sites on the H/Si surface. For example, in work by Hines and co-workers,[12] analysis of the integrated infrared intensities in the ν(Si−H) region for H/Si(111) after exposure to O_2-saturated water seemingly indicated an increase in surface hydrogens, which they attributed to a roughened surface morphology. However, such interpretations rely heavily on the ν(Si−H) dipole moment derivatives being similar for H/Si and H/SiO_n species. This may not be a reasonable assumption due to inductive effects on the Si−H dynamic dipole due to neighboring oxygens, which have an electronegativity larger than silicon by a factor of ∼2.

In the present work, first-principles calculations based on density functional theory are carried out on cluster models representing the H-terminated Si(100)-2×1 surface to investigate the effect of oxygen incorporation on the infrared intensities of ν(Si−H) for pristine and oxidized H/Si surfaces. Comparisons are made between results obtained for a pristine H/Si surface site and surface sites containing one to five oxygen atoms incorporated into the Si−Si back and dimer bonds, representing maximum agglomeration.

II. Computational Details

As in previous theoretical studies, a silicon cluster is used in this work to represent a dimer site on the Si surface.[1,3−7,15,16] The cluster model corresponds roughly to one unit cell of the 2×1 reconstructed H/Si(100) surface, consisting of nine silicon atoms. The starting geometry for the model surface site corresponds to an ideal tetrahedral configuration, generated by setting each Si−Si bond length to 2.35 Å, with the usual interatomic angle of 109.47°. The cluster is terminated by hydrogen atoms to satisfy the valency of the cleaved Si−Si bonds during excision from the extended surface, giving a cluster stoichiometry of Si_9H_{14}. Boundary constraints, fixing atoms to

* Corresponding author. E-mail: kraghava@indiana.edu.

10.1021/jp046808d CCC: $27.50
Published on Web 11/18/2004

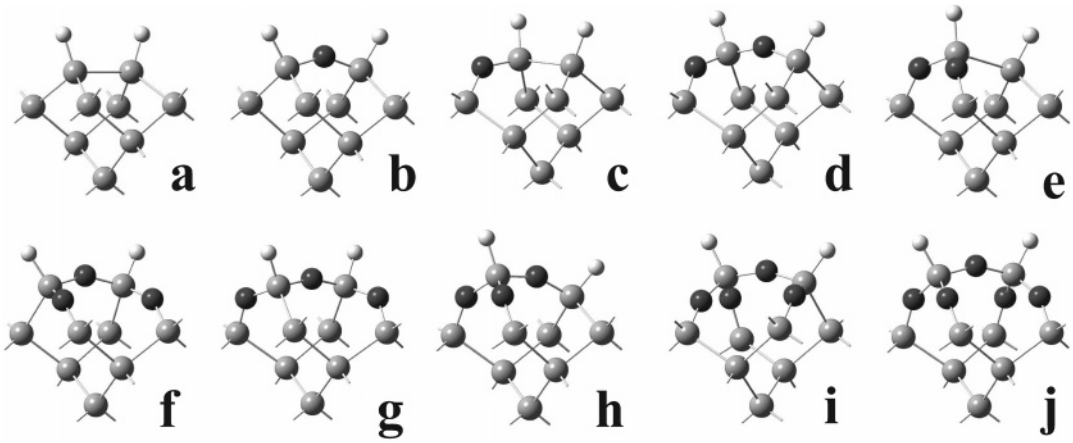

Figure 1. The B3-LYP/*dz*P optimized Si_9 cluster models of the pristine and multiply oxidized H/Si(100)-2×1 surface used to calculate the infrared intensities in this study: ranging from (a) the pristine unoxidized surface site to (j) the fully agglomerated surface site incorporating five oxygens into the Si−Si dimer and back-bonds. (Terminal hydrogens are omitted for clarity.)

Cartesian coordinates specified by their bulk tetrahedral positions, are imposed on the third- and fourth-layer Si atoms to avoid unphysical structural relaxation. The terminal hydrogens that replace third- or deeper layer silicons are also held fixed in their Cartesian positions, which correspond to an Si−H distance of 1.48 Å along ideal tetrahedral directions. The other atoms in the cluster, including the added oxygens, are allowed to move freely to minimize the system energy. In the discussion that follows, the surface cluster model orientation is such that the *x*-axis lies along a dimer row, the *y*-axis is perpendicular to a dimer row, requiring the *z*-axis to be normal to the H/Si surface. The calculations presented here were performed using the Gaussian 03 suite of electronic structure programs[17] using the B3-LYP hybrid density functional, which corresponds to Becke's three-parameter exchange functional (B3)[18] along with the Lee−Yang−Parr gradient-corrected correlation functional (LYP).[19] A multilevel polarized and augmented basis set of double-ζ quality (denoted here as *dz*P) was employed in this work, representing the surface hydrogens and first-layer atoms with the 6-31+G(3df,3pd) basis set, the second layer silicons with the 6-31G(d) basis set, and the lower layer frozen cluster atoms with the 6-31G basis set.[20,21] Minimum energy structures, subject to the Si cluster boundary constraints, were calculated for the pristine surface dimer model and oxidized dimer cluster models having stoichiometries of $Si_9H_{14}O_n$ ($n = 1-5$). Following structural optimizations, harmonic vibrational frequencies and dipole moment derivatives were calculated analytically. The application of structural constraints to mimic the mechanical effect of the extended surface introduces artificial forces that must be properly accounted for in the gas-phase cluster frequency calculations. In this work, this is treated in a consistent manner by assigning infinite masses to the fixed atoms in building the mass-weighted Hessian. Isotropic ν(Si−H) infrared intensities were computed from the dipole moment derivatives in the double harmonic approximation.[22] The fixed cluster orientation allows the calculation of approximate surface infrared intensities by considering only the $\partial\mu/\partial Q_Z$ dipole moment derivative components. Atomic charges were calculated using the Natural Population Analysis scheme of NBO version 3.[23−27]

III. Results and Discussion

The prediction of quantitatively reliable infrared intensities requires significantly larger basis sets than are typically used to calculate structure and energetics for chemical systems, such as the *dz*P basis set employed here. The need for highly polarized basis sets augmented by the addition of diffuse functions when predicting infrared intensities is attributed to the added flexibility they lend to the electronic wave function, allowing it to deform in the presence of an electric field.[28,29] Previous work by Halls and Schlegel[30] has shown that hybrid density functional methods (e.g., B3-LYP) perform very well in comparison to conventional quantum chemical approaches such as Hartree−Fock, second-order Møller−Plesset perturbation theory (MP2), and quadratic configuration interaction with single and double excitations (QCISD) in predicting quantitative infrared intensities.

The cluster models representing the pristine and oxidized H/Si(100)-2×1 surface sites are shown in Figure 1. The starting point for the current discussion is the pristine H/Si surface site, cluster a, which in the theoretical chemistry community is the most often used model of the H/Si(100)-2×1 surface. From there, nine other cluster models have been explored, systematically incorporating one to five oxygens into the silicon lattice of the surface unit cell with various structural configurations b−j. The B3-LYP/*dz*P results for clusters a−j are presented in Table 1, including the ν(Si−H) harmonic frequencies, infrared intensities, atomic charges, and geometric Si−H bond lengths. Experimental infrared studies on H/Si surfaces are often carried out with geometric considerations or buried metallic layers to increase the sensitivity to vibrational modes with transition dipoles normal to the H/Si surface.[1,10] Therefore, perhaps most importantly, also in Table 1 are the surface infrared intensities computed considering only the dipole moment derivatives perpendicular to the H/Si surface, along with the angle between the Si−H bond and the surface normal for discussion purposes. It should be noted that each cluster contains two surface hydrogen atoms whereas only one is listed in Table 1. In all cases, we focus on the hydrogen with the larger number of neighboring oxygens in Table 1. To illustrate the intrinsic effects of the environment on the computed frequencies, we have deuterated the other surface hydrogen to decouple the vibrational modes. This yields the intrinsic or "isolated" frequencies listed in Table 1. For example, considering the −HSi−SiH− cluster a model first, the two raw (unscaled) computed ν(Si−H) vibrational frequencies are 2177 (antisymmetric) and 2185 (symmetric) cm^{-1}. The splitting between the two modes as well as their polarizations are in excellent agreement with the corresponding experimental observations. The corresponding intrinsic or isolated frequency is computed to be 2181 cm^{-1} (computed from −HSi−SiD−, which yields the average fre-

TABLE 1: B3-LYO/*dxP* Calculated ν(Si−H) Vibrational Frequencies, Normal Angle, Bond Length, Atomic Charges, and Infrared Intensities for the Pristine and Oxidized Hydrogen-Terminated Si(100)-2×1 Surface Structures (Shown in Figure 1)

	structure	ν(Si−H)[a] (cm^{-1})	∠(Si−H *z*) (deg)	*R* Si−H (Å)	q[b] Si	q[b] H	I_{IR} (km/mol) isotropic	I_{IR} (km/mol) surface	% *z* change
a	−HSi−SiH−	2181	19.4	1.49	−0.02	−0.12	111.7	92.0	0%
b	−HSi−O−SiH−	2199	32.8	1.48	0.87	−0.19	150.8	105.2	14%
c	−O−HSi−SiH−	2195	18.1	1.48	0.94	−0.19	142.1	126.3	37%
d	−O−HSi−O−SiH−	2240	27.5	1.48	1.64	−0.24	173.8	141.2	54%
e	−O−(−O−)HSi−SiH−	2240	5.7	1.48	1.68	−0.23	162.9	149.0	62%
f	−O−HSi−O−SiH−O−	2240	32.7	1.48	1.63	−0.24	182.7	134.1	46%
g	−O−HSi−O−SiH−O′−	2239	30.5	1.48	1.64	−0.24	167.7	130.3	42%
h	−O−(−O−)HSi−O−SiH−	2329	18.8	1.46	2.22	−0.26	132.0	113.8	24%
i	−O−(−O−)HSi−O−SiH−O−	2327	24.8	1.46	2.22	−0.26	133.8	106.7	16%
j	−O−(−O−)HSi−O−SiH(−O−)−O−	2328	31.4	1.46	2.22	−0.26	134.0	95.8	4%

[a] Unscaled harmonic vibrational frequencies. [b] Atomic charges computed using the National Population Analysis scheme of NBO version 3.

quency, as expected). Due to incomplete treatment of electron correlation, neglect of mechanical anharmonicity, and basis set truncation effects, calculated harmonic frequencies generally overestimate experimental wavenumbers. To improve the agreement between the predicted and observed frequencies, the computed harmonic frequencies are usually scaled for comparison. A detailed study of B3-LYP frequencies obtained with a spectroscopic basis set,[31] similar to *dz*P used here, suggests a scaling factor of 0.96 which would yield a corrected ν(Si−H) frequency of 2094 cm^{-1}, in close agreement with experimental observations.[10] The Si−H bond is found to have a length of 1.49 Å and makes an angle of 19.4° with the surface normal. The isotropic ν(Si−H) infrared intensity for the −HSi−SiH− model is 111.7 km/mol. The relative surface intensities between the pristine and oxidized clusters can be understood in terms of geometric and electronic factors. An increase in infrared intensity can occur either due to enhanced coupling of the dynamic dipole with the incident radiation field, which would correspond to a smaller difference between the angle made between the surface and the Si−H linkage and 90°, or due to an increase in the dynamic dipole, which is reflected in the Si−H distance and the Si/H effective atomic charges. The reference surface infrared intensity for ν(Si−H) is calculated to 92.0 km/mol.

Singly oxidized H/Si(100)-2×1 surface sites can incorporate oxygen into the top Si−Si dimer bond, producing the −HSi−O−SiH− cluster (b) or the back Si−Si bond producing the −O−HSi−SiH− cluster (c). Upon the incorporation of a single O into the H/Si surface site, the ν(Si−H) vibration is shifted higher by ca. 14−18 cm^{-1}. For both singly oxidized surface sites, the Si−H bond distance is 1.48 Å, which is slightly contracted from the reference Si−H bond length. Considering the atomic charges in Table 1, the electronic effect can be seen in the differences in Si and H atomic charges upon O incorporation. In both clusters b and c, the atomic charges indicate an increase in polarization along the Si−H bond. In the oxidized dimer bond cluster (b), the isotropic and surface infrared intensities are 150.8 and 105.2 km/mol, respectively. The ν(Si−H) surface infrared intensity is increased by 14% upon insertion of an oxygen into the Si−Si dimer bond. The oxidized back-bond cluster (c) has a surface infrared intensity that is enhanced by 37% over the pristine −HSi−SiH− model, with I_Z^{IR} = 126.3 km/mol. Comparison of the results obtained for the −HSi−O−SiH− and −O−HSi−SiH− models shows that, despite experiencing similar electronic effects due to incorporation of oxygen, cluster c has a larger surface intensity due to the geometric factor with its Si−H bond making an angle of 18.1° with the surface normal, which is 14.7° more favorable than the oxidized dimer site and is within ca. 1° from the reference geometry.

Cluster models d and e represent doubly oxidized surface sites in which oxygen is incorporated into both the Si−Si dimer and the back-bonds producing the −O−HSi−O−SiH− cluster (d), or into both back-bonds on one side of the Si−Si dimer producing the −O−(O)−HSi−SiH− cluster (e). For both doubly oxidized sites, the ν(Si−H) vibration is upshifted by 59 cm^{-1}. The Si−H bond length is conserved from the singly oxidized species, and the Si/H atomic charges for the doubly oxidized clusters are comparable. The isotropic intensities for clusters d and e are calculated to be 173.8 and 162.9 km/mol, respectively. The −O−HSi−O−SiH− cluster (d) has a surface infrared intensity of 141.2 km/mol, which is 54% larger than the pristine −HSi−SiH− site (a). This is quite significant because it, along with b and c, has been identified as a dominant surface species in oxidation studies of the H/Si(100)-2×1 surface (see, for example, ref 10). The doubly oxidized back-bond cluster e has a surface infrared intensity of 149.0 km/mol, which is even larger than that of cluster d, due to the geometric factor having a ∠(Si−H *z*) of only 5.7°. Of all of the surface site models considered in this study, cluster e has the most favorable geometric factor for surface infrared absorption with a Si−H oscillator in maximum coincidence with the normal component of the electric field at the surface.

An increase in the number of oxygens per surface unit to three leads to the triply oxidized cluster models f, g, and h, shown in Figure 1. The properties of structures f and g (−O−HSi−O−SiH−O−) are similar to those of the doubly oxidized cluster d (−O−HSi−O−SiH−), because there are only two neighboring oxygens per surface Si−H. The isotropic infrared intensities for f and g are 182.7 and 167.7 km/mol, respectively. The surface infrared intensities are 46% and 42% larger than the unoxidized site, being 134.1 and 130.3 km/mol for f and g. Cluster surface model h is also a triply oxidized cluster; however, it is different in that the three oxygens are clustered around a single surface Si−H. The ν(Si−H) frequency for surface sites represented by cluster h is 148 cm^{-1} higher than the reference cluster mode and has been observed experimentally as a minor species.[11] In addition to a greatly increased ν(Si−H) frequency, the effect of having three neighboring atoms with greater electronegativity is evident from the Si−H bond length, which is contracted further to 1.46 Å, and from a sizable increase in Si atomic charge. The −O−(O)−HSi−O−SiH− cluster has an isotropic infrared intensity of 132.0 km/mol and a polarized surface absorption of 113.8 km/mol, which is enhanced by 24%.

The final surface sites considered in this work incorporate four and five oxygens into the surface unit cell lattice, which would represent maximum oxygen agglomeration. The −O−(O)−HSi−O−SiH−O− and −O−(O)−HSi−O−SiH−(O)−O− surface cluster models are shown in Figure 1, as i and j, respectively. As found when comparing the results for clusters

f and g with d, the properties of clusters i and j resemble those of cluster h, because all have three nearest neighbor oxygens. Inspection of the results in Table 1 shows that, although h, i, and j have an identical Si−H bond length, similar electronic properties (e.g., Si/H atomic charges), and isotropic infrared intensities, their surface infrared intensities differ by up to 18 km/mol. This is attributable to differing geometric factors with $\angle$(Si−H z) having values of 18.8°, 24.8°, and 31.4° for the h, i, and j oxidized surface sites.

The results presented here illustrate that, contrary to a common assumption, ν(Si−H) band intensities are quite sensitive to oxygen incorporation into the surface Si lattice structure, with both the isotropic and the surface infrared absorption increasing significantly. The effect of oxygen insertion on infrared intensities stems from an interplay of geometric and electronic effects at the surface Si−H site. For the single (b and c) and double oxygen inserted surface dimer sites (d and e), an increase in surface infrared absorption (I_Z^{IR}) from 14% to 37% and 54% to 62% is predicted, respectively. Experimental infrared investigations using the ν(Si−H) spectral region to track changes in hydrogen monolayer coverage and extract information related to chemical reaction mechanisms upon exposure of H/Si surfaces to various oxygen contained precursors may have to be revisited in light of this work.

Given the magnitude and significance of the effect of oxidation on silicon surface site infrared intensities, further investigations are warranted. In particular, the use of larger cluster models of the Si(100)-2×1 surface may yield more quantitative estimates of the changes in infrared adsorption. A cost-effective approach to studying the vibrational properties of larger fragments of the Si(100)-2×1 surface may be the QM/MM embedded cluster method, treating one region with a higher accuracy quantum mechanical (QM) method and the rest represented inexpensively using molecular mechanics (MM). However, response properties from such composite methods have not yet been validated, and their performance is unknown. For such studies, new molecular mechanics force fields may be required, or existing ones refined, with such considerations as ensuring that the atomic charges closely mimic the atomic polar tensors for the system under study.

Acknowledgment. We gratefully acknowledge computational resources provided by the University Information Technology Services (UITS), Indiana University, and from NCSA (Grant No. CHE030049). M.D.H. would also like to thank the Department of Chemistry, Indiana University, for financial support provided by an Ernest R. Davidson postdoctoral fellowship. We are grateful to Y. J. Chabal, Rutgers University, for insightful discussions.

References and Notes

(1) Chabal, Y. J.; Harris, A. L.; Raghavachari, K.; Tully, J. C. *Int. J. Mod. Phys. B* **1993**, *7*, 1031.

(2) Yablonovitch, E.; Allara, D. L.; Chang, C. C.; Gmitter, T.; Bright, T. B. *Phys. Rev. Lett.* **1988**, *53*, 998.

(3) Trucks, G. W.; Raghavachari, K.; Higashi, G. S.; Chabal, Y. J. *Phys. Rev. Lett.* **1990**, *65*, 504.

(4) Chabal, Y. J.; Raghavachari, K. *Surf. Sci.* **2002**, *502*−*503*, 41.

(5) Chabal, Y. J.; Raghavachari, K. *Phys. Rev. Lett.* **1984**, *53*, 282.

(6) Chabal, Y. J.; Raghavachari, K. *Phys. Rev. Lett.* **1985**, *54*, 1055.

(7) Chabal, Y. J.; Higashi, G. S.; Raghavachari, K.; Burrows, V. A. *J. Vac. Sci. Technol.* **1989**, *A7*, 2104.

(8) Raghavachari, K.; Jakob, P.; Chabal, Y. J. *Chem. Phys. Lett.* **1993**, *206*, 156.

(9) *Proceedings of the 1st*−*3rd International Symposium on the Physics and Chemistry of SiO_2 and the Si/SiO_2 Interface*; Massoud, H. Z., Poindexter, E. H., Helms, C. R., Eds.; Electrochemical Society: Pennington, NJ, 1988−1996; Vol. 3.

(10) Weldon, M. K.; Stefanov, B. B.; Raghavachari, K.; Chabal, Y. J. *Phys. Rev. Lett.* **1997**, *79*, 2851.

(11) Weldon, M. K.; Queeney, K. T.; Gurevich, A. B.; Stevanov, B. B.; Chabal, Y. J.; Raghavachari, K. *J. Chem. Phys.* **2000**, *113*, 2440.

(12) Garcia, S. P.; Bao, H.; Manimaran, M.; Hines, M. A. *J. Phys. Chem. B* **2002**, *106*, 8258.

(13) Cui, Z. J.; Takoudis, C. G. *J. Electrochem. Soc.* **2003**, *150*, G694.

(14) Niwano, M.; Kageyama, J.; Kinashi, K.; Miyamoto, N.; Honma, K. *J. Vac. Sci. Technol.* **1994**, *A12*, 465.

(15) Raghavachari, K.; Chabal, Y. J.; Struck, L. M. *Chem. Phys. Lett.* **1996**, *252*, 230.

(16) Struck, L. M.; Eng, J.; Bent, B. E.; Flynn, G. W.; Chabal, Y. J.; Christman, S. B.; Chabal, E. E.; Raghavacahri, K.; Williams, G. P.; Rademacher, K.; Mantl, S. *Surf. Sci.* **1997**, *380*, 444.

(17) Frisch, M. J.; Trucks, G. W.; Schlegel, H. B.; Scuseria, G. E.; Robb, M. A.; Cheeseman, J. R.; Montgomery, J. A., Jr.; Vreven, T.; Kudin, K. N.; Burant, J. C.; Millam, J. M.; Iyengar, S. S.; Tomasi, J.; Barone, V.; Mennucci, B.; Cossi, M.; Scalmani, G.; Rega, N.; Petersson, G. A.; Nakatsuji, H.; Hada, M.; Ehara, M.; Toyota, K.; Fukuda, R.; Hasegawa, J.; Ishida, M.; Nakajima, T.; Honda, Y.; Kitao, O.; Nakai, H.; Klene, M.; Li, X.; Knox, J. E.; Hratchian, H. P.; Cross, J. B.; Adamo, C.; Jaramillo, J.; Gomperts, R.; Stratmann, R. E.; Yazyev, O.; Austin, A. J.; Cammi, R.; Pomelli, C.; Ochterski, J. W.; Ayala, P. Y.; Morokuma, K.; Voth, G. A.; Salvador, P.; Dannenberg, J. J.; Zakrzewski, V. G.; Dapprich, S.; Daniels, A. D.; Strain, M. C.; Farkas, O.; Malick, D. K.; Rabuck, A. D.; Raghavachari, K.; Foresman, J. B.; Ortiz, J. V.; Cui, Q.; Baboul, A. G.; Clifford, S.; Cioslowski, J.; Stefanov, B. B.; Liu, G.; Liashenko, A.; Piskorz, P.; Komaromi, I.; Martin, R. L.; Fox, D. J.; Keith, T.; Al-Laham, M. A.; Peng, C. Y.; Nanayakkara, A.; Challacombe, M.; Gill, P. M. W.; Johnson, B.; Chen, W.; Wong, M. W.; Gonzalez, C.; Pople, J. A. *Gaussian 03*, revision B.2; Gaussian, Inc.: Pittsburgh, PA, 2003.

(18) Becke, A. D. *J. Chem. Phys.* **1993**, *98*, 5648.

(19) Lee, C.; Yang, W.; Parr, R. G. *Phys. Rev. B* **1988**, *37*, 785.

(20) Hariharan, P. C.; Pople, J. A. *Theor. Chim. Acta* **1973**, *28*, 213.

(21) Francl, M. M.; Petro, W. J.; Hehre, W. J.; Binkley, J. S.; Gordon, M. S.; DeFrees, D. J.; Pople, J. A. *J. Chem. Phys.* **1982**, *77*, 3654.

(22) Overend, J. In *Infrared Spectroscopy and Molecular Structure*; Davies, M., Ed.; Elsevier Scientific: Amsterdam, 1963; p 345.

(23) Carpenter, J. E.; Weinhold, F. *J. Mol. Struct. (THEOCHEM)* **1988**, *169*, 41.

(24) Foster, J. P.; Weinhold, F. *J. Am. Chem. Soc.* **1980**, *102*, 7211.

(25) Reed, A. E.; Weinhold, F. *J. Chem. Phys.* **1983**, *78*, 4066.

(26) Reed, A. E.; Weinstock, R. B.; Weinhold, F. *J. Chem. Phys.* **1985**, *83*, 735.

(27) Reed, A. E.; Curtiss, L. A.; Weinhold, F. *Chem. Rev.* **1988**, *88*, 899.

(28) Werner, H. J.; Meyer, W. *Mol. Phys.* **1976**, *31*, 855.

(29) Dierksen, G. H. F.; Sadlej, A. J. *Theor. Chim. Acta* **1983**, *63*, 69.

(30) Halls, M. D.; Schlegel, H. B. *J. Chem. Phys.* **1998**, *109*, 10587.

(31) Halls, M. D.; Velkovski, J.; Schlegel, H. B. *Theor. Chem. Acc.* **2001**, *105*, 413.